ACS APPLIED MATERIALS & INTERFACES

Research Article

Cite This: ACS Appl. Mater. Interfaces 2018, 10, 1217−1224

www.acsami.org

High Dynamic Range (Δn) Two-Stage Photopolymers via Enhanced Solubility of a High Refractive Index Acrylate Writing Monomer

Marvin D. Alim,[†] David J. Glugla,[‡] Sudheendran Mavila,[§] Chen Wang,[§] Philip D. Nystrom,[∥] Amy C. Sullivan,[‡] Robert R. McLeod,*[,†,‡] and Christopher N. Bowman*[,†,§]

[†]Materials Science and Engineering Program, UCB 596, [‡]Department of Electrical, Computer, and Energy Engineering, UCB 425, [§]Department of Chemical and Biological Engineering, UCB 596, and [∥]Department of Mechanical Engineering, UCB 427, University of Colorado Boulder, Boulder, Colorado 80309, United States

Supporting Information

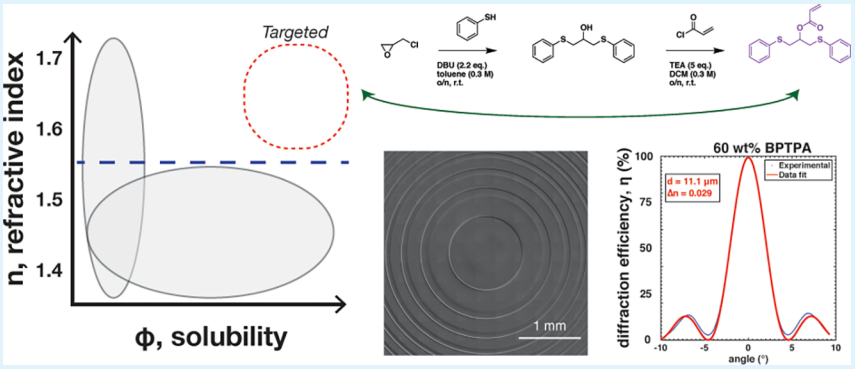

ABSTRACT: Holographic photopolymers capable of high refractive index modulation (Δn) on the order of 10^{-2} are integral for the fabrication of functional holographic optical elements that are useful in a myriad of optical applications. In particular, to address the deficiency of suitable high refractive index writing monomers for use in two-stage holographic formulations, here we report a novel high refractive index writing monomer, 1,3-bis(phenylthio)-2-propyl acrylate (BPTPA), simultaneously possessing enhanced solubility in a low refractive index (n = 1.47) urethane matrix. When examined in comparison to a widely used high refractive index monomer, 2,4,6-tribromophenyl acrylate, BPTPA exhibited superior solubility in a stage 1 urethane matrix of approximately 50% with a 20% higher refractive index increase per unit amount of the writing monomer for stage 2 polymerizations. Formulations with 60 wt % loading of BPTPA exhibit a peak-to-mean holographic $\Delta n \approx 0.029$ without obvious deficiencies in transparency, color, or scatter. To the best of our knowledge, this value is the highest reported in the peer-reviewed literature for a transmission hologram. The capabilities and versatility of BPTPA-based formulations are demonstrated at varying length scales via demonstrative refractive index gradient structure examples including direct laser write, projection mask lithography of a 1″ diameter Fresnel lens, and ∼100% diffraction efficiency volume transmission holograms with a 1 μm fringe spacing in 11 μm thick samples.

KEYWORDS: *holography, two-stage photopolymer, high Δn, refractive index gradient structures, Fresnel lens*

1. INTRODUCTION

Two-stage photopolymers are an ideal framework for designing materials capable of accessing a wide range of material properties (mechanical, thermal, optical, electrical, etc.) on demand using light.[1−3] A valuable implementation of the two-stage paradigm is in designing recording materials (often referred to as holographic photopolymers[4−13]) for appropriate refractive index (phase) structures using various optical exposure techniques (such as photolithography,[14] direct laser write (DLW),[15] two-photon lithography,[16] and holography[4−13]) to generate a refractive index contrast (Δn) between the bulk material and the recorded feature(s). In particular, the advent of augmented reality devices has spurred a rising interest to use photopolymers to fabricate holographic optical elements (HOEs) capable of complex, yet high quality, optical functions with thin, light, and flexible form factors.[17]

The general scheme involves an initial thermal cure of a solid rubbery matrix (stage 1), typically of lower refractive index (n < 1.5). This matrix acts as a framework through which dissolved species (writing monomer and photoinitiator) freely diffuse and undergo photopolymerization during a subsequent patterned irradiation step. This patterned light exposure spatially controls the polymerization (stage 2) according to the light intensity profile, consuming the reactive monomer species in the exposed regions and inducing mass transport of

Received: October 4, 2017
Accepted: December 13, 2017
Published: December 13, 2017

DOI: 10.1021/acsami.7b15063
ACS Appl. Mater. Interfaces 2018, 10, 1217−1224

the additional monomer from the unexposed regions into the exposed regions to enhance the developing refractive index structure. The net outcome is a phase structure that ideally corresponds directly to the exposure pattern recorded in a thin, transparent polymeric film. The primary development goal for practical application is to maximize the material's available dynamic range, that is, the achievable Δn as this enables a significant enhancement in diffraction efficiency for a given thickness and number of recordable multiplexed holograms.[18] A higher Δn also enables the manufacture of gradient refractive index (GRIN) lenses with greater focusing power as well as having the capacity to record waveguides with tighter bend radii. In terms of device performance, this translates to improved specifications such as wider field of views, higher information densities, lower power readout sources, and so forth.

Within the scope of formulating two-stage holographic photopolymers, the recordable Δn is a function of the difference in refractive index of the writing polymer and the matrix ($n_{polymer} - n_{matrix}$) as well as the volume fraction of the initial writing monomer present in the material ($\varnothing$).[19] However, effective high refractive index substituents (such as heavy halogens or aromatics[20−22]) have high molar refractions and low molar volumes, which are drastically different in structure, compared to the substituents of lower refractive index.[20,22,23] Therefore, for a given matrix, there is typically a significant trade-off between increasing the refractive index of the writing monomer and its reduced solubility in the underlying matrix.

Recently, sequential and orthogonal two-stage thiol-X click chemistry systems achieving high solubility have been successfully demonstrated with simple processability;[7,8] however, these formulations exhibited a low overall Δn ($\leq 4.0 \times 10^{-3}$) primarily because of the low refractive index difference ($n_{polymer} - n_{matrix}$) associated with the presence of thiols in stage 1 reactions. Similar issues of limited achievable Δn are encountered with alternative photopolymer systems involving acrylamide writing monomers,[24,25] which have refractive indices similar to those of the binder, poly(vinyl alcohol).[9] Other groups have explored holographic composites such as nanoparticle-based photopolymers or liquid-crystal photopolymers whereby the nanoparticles or liquid crystals,[26−30] acting as nonreactive higher refractive index species, migrate to the dark regions upon holographic exposure.[10,11,31] Notably, Tomita et al. reported a peak-to-mean Δn of 0.022 using high refractive index hyperbranched organic nanoparticles[11] (hitherto, the highest reported for materials in the academic literature). However, the intrinsic drawbacks of limited nanoparticle solubility and the slow reaction kinetics (>1 min for Δn development despite high recording intensities of 100−200 mW/cm^2) persist. The synthesis of high refractive index nanoparticles is also relatively cumbersome and arguably not a viable approach for mass use as recording materials in the aforementioned applications. Recently, Covestro AG have commercialized a product line of holographic photopolymer materials, Bayfol HX, capable of high Δn values of up to 0.035 for reflection holograms at approximately 220 nm. However, at higher pitch recordings, there is a noticeable decrease in Δn with a reported value of less than 0.01 for a 1 μm grating.[32]

Here, a stage 1 urethane and stage 2 acrylate formulation, similar to existing commercial materials,[32,33] were combined to yield superior orthogonality and Δn recording performance relative to most other two-stage formulation systems. Focusing on maximizing the solubility of the writing monomer in a urethane matrix without reducing the Δn, a colorless, low viscosity, high refractive index (n_D = 1.6) liquid acrylate monomer, 1,3-bis(phenylthio)-2-propyl acrylate (BPTPA), was designed and synthesized using a facile synthetic route involving only two relatively simple steps. Solubility and refractive index experiments were performed to evaluate viability as a two-stage holographic writing monomer against a reference, a widely used high refractive index monomer, 2,4,6-tribromophenyl acrylate (TBPA).[1,19] Monomer swelling studies of a urethane matrix showed a solubility improvement of around 50% as compared to TBPA in addition to a moderately higher refractive index increase per unit concentration of the writing monomer. Crucially, we demonstrate that optically clear films containing twice the amount of the writing monomer are possible with BPTPA (60 wt %) when compared to TBPA, making peak-to-mean $\Delta n \approx 0.029$ accessible without any discernible optical deficiencies. To the best of our knowledge, this is the highest Δn for any reported holographic photopolymer within the peer-reviewed, that is, nonpatent, literature. The capabilities and versatility of BPTPA formulations are demonstrated through functional examples of refractive index structures at varying length scales through DLW of an intricate pattern, the projection mask lithography of a Fresnel lens, and transmission holograms.

2. EXPERIMENTAL SECTION

Commercially available reagents were used without further purification. Thiophenol, epichlorohydrin, and butylated hydroxytoluene (BHT) free radical stabilizer were purchased from Alfa Aesar. 1,8-Diazabicyclo[5.4.0]undec-7-ene (DBU) was purchased from Chem Impex International. 4-Dimethylaminopyridine (DMAP) was purchased from Oakwood Chemicals. Reagent-grade triethylamine (Et_3N) was purchased from Fisher Scientific. Acryloyl chloride and polycaprolactone-*block*-polytetrahydrofuran-*block*-polycaprolactone (average M_n 2000) were purchased from Sigma-Aldrich. The photoinitiator, diphenyl(2,4,6-trimethylbenzoyl)phosphine oxide (TPO), was purchased from TCI America. Desmodur N3900 polyisocyanate was donated by Covestro AG (formerly Bayer MaterialScience).

2.1. Monomer Synthesis. *2.1.1. Synthesis of 1,3-Bis-(phenylthio)-2-propanol (BPTP).* To a 250 mL round-bottomed flask equipped with a magnetic stir bar, 16 mL of thiophenol (157 mmol, 2.2 equiv) was stirred with 23 mL of DBU (154 mmol, 2.2 equiv) in 230 mL of toluene (0.3 M, wrt epichlorohydrin) for 10 min. Following this, 5.5 mL of epichlorohydrin (70.3 mmol, 1.0 equiv) was added dropwise. The reaction vessel was allowed to stir at room temperature for 16 h. After this period, the volatiles were removed under reduced pressure, and the residue was then diluted with dichloromethane (DCM) and washed with 1 M HCl (100 mL), distilled water (100 mL), and brine (50 mL). The combined organic extracts were dried over anhydrous Na_2SO_4, filtered, and concentrated under reduced pressure. The crude product was purified by silica-gel column chromatography using 20% EtOAc in hexane as an eluent to yield 17.1 g of a colorless, low viscosity liquid (88% yield).

^{1}H NMR (400 MHz, $CDCl_3$): δ 7.36−7.33 (m, 4H), 7.29−7.24 (m, 4H), 7.22−7.18 (m, 2H), 3.86−3.79 (m, 1H), 3.20 (dd, J = 13.8, 5.0 Hz, 2H), 3.05 (dd, J = 13.8, 7.2 Hz, 2H), 2.74 (bs, 1H).

^{13}C NMR (101 MHz, $CDCl_3$, 25 °C): δ 135.1, 129.9, 129.1, 126.7, 68.2, 40.1.

2.1.2. Synthesis of Acrylate Writing Monomer, BPTPA. To a 250 mL round-bottomed flask equipped with a magnetic stir bar, 10 g of BPTP (36.2 mmol, 1.0 equiv), 25.2 mL of Et_3N (180.9 mmol, 5 equiv), and 0.4 g of BHT (1.81 mmol, 0.05 equiv) were diluted with 120 mL of DCM (0.3 M wrt BPTP) and stirred for 10 min under argon atmosphere. The clear solution was cooled to 0 °C, and 4.4 mL of acryloyl chloride (54.3 mmol, 2.2 equiv) was added dropwise to the

DOI: 10.1021/acsami.7b15063
ACS Appl. Mater. Interfaces 2018, 10, 1217−1224

Scheme 1. (a) Overall Synthetic Route for Novel Acrylate Writing Monomer, BPTPA. The Intermediate Alcohol, BPTP, Is Synthesized by Reaction with Excess Thiol under Basic Conditions To Favor the Bifunctional Substitution after the Thiol−Epoxy Ring-Opening Reaction; (b) Schematic Illustration for Two-Stage Holographic Photopolymer Formulations. The Stage 1 Alcohol−Isocyanate Network Is Thermally Cured at 70 °C Overnight with the Dissolved Writing Chemistry (TPO Photoinitiator with Either TBPA or BPTPA) Available for 405 nm Recording

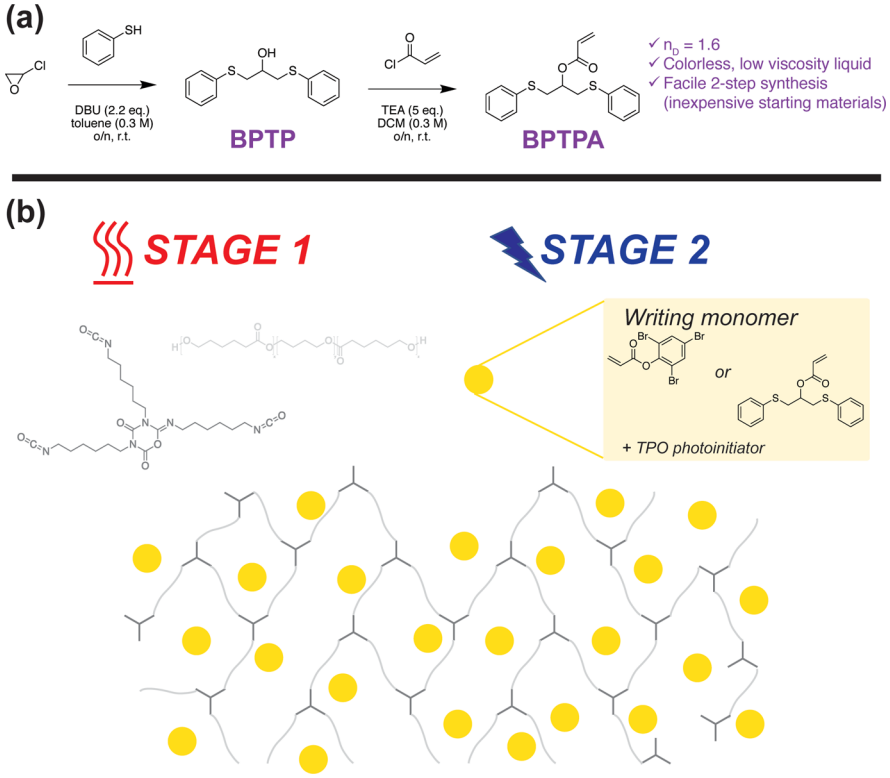

flask under Ar atmosphere followed by 0.4 g of DMAP (3.6 mmol, 0.1 equiv). The reaction mixture was allowed to stir at room temperature for 16 h. After this period, the volatiles were removed under reduced pressure, and the residue was diluted with DCM (250 mL) and washed with 1 M HCl (100 mL), distilled water (100 mL), and brine (50 mL). The combined organic extracts were dried over anhydrous Na_2SO_4, filtered, and concentrated under reduced pressure. The crude product was purified by silica-gel column chromatography using 20% EtOAc in hexane as an eluent to yield the title compound BPTPA as a colorless, low viscosity liquid (84% yield).

^{1}H NMR (400 MHz, $CDCl_3$): δ 7.38−7.35 (m, 4H), 7.28−7.24 (m, 4H), 7.20−7.16 (m, 2H), 6.27 (dd, J = 17.3, 1.4 Hz, 1H), 5.94 (dd, J = 17.3, 10.5 Hz, 1H), 5.76 (dd, J = 10.5, 1.4 Hz, 1H), 5.18 (p, J = 5.9 Hz, 1H), 3.29 (dd, J = 5.9, 3.3 Hz, 4H).

^{13}C NMR (101 MHz, $CDCl_3$, 25 °C): δ 165.3, 135.2, 131.4, 129.9, 129.0, 127.9, 126.6, 72.0, 36.3.

2.2. Nuclear Magnetic Resonance (NMR). NMR spectra were recorded on a Bruker AVANCE-III 400 NMR spectrometer at 25 °C in chloroform-*d*. All chemical shifts are reported in ppm relative to the chloroform solvent peak (δ = 7.26 ppm).

2.3. Refractive Index Measurements. The refractive indices of liquid samples were measured using an Abbe refractometer at the sodium-d line (589.3 nm) at room temperature. The refractive index of polymeric films was measured using a Metricon 2010/M prism coupler at a wavelength of 633 nm under ambient conditions.

2.4. Writing Monomer Swelling in a Urethane Matrix. Half-inch diameter disks were punched out of 250 μm urethane films, and their dry weights (W_i) were measured. They were then individually placed in 4 mL vials containing (a) 20 wt % TBPA in solvent, (b) 20 wt % BPTPA in solvent, or (c) 100% solvent. The relatively nonvolatile "solvent" chosen was heavy mineral oil. After 1 week, the surface of each disk was patted dry with a weighing paper, and their equilibrium weights (W_f) were measured.

2.5. Two-Stage Photopolymer Recording Film Preparation. Two-stage photopolymer film samples were prepared by premixing the acrylate writing monomer (either TBPA or BPTPA) measured at a set weight percentage (relative to the entire formulation) with 1−3 wt % TPO photoinitiator (based on the writing monomer concentration) and the difunctional polyol in a 4 mL vial equipped with a magnetic stir bar until homogeneous. A stoichiometric amount (OH/NCO = 1:1) of Desmodur N3900 trifunctional isocyanate was added to the vial and stirred. The resin was cast onto clean 1 × 1.5″ glass slides and sandwiched with a corresponding glass slide or cover slip (Fisher Scientific) using binder clips with polyethylene terephthalate spacers of defined thicknesses (15, 25, and 250 μm) lining the perimeter to control the thickness. Samples were covered with aluminum foil and allowed to cure overnight in an oven at 70 °C. Acrylate reactivity was confirmed via Fourier transform infrared spectroscopy (FTIR) to be negligible throughout this thermal process. A representation of the two-stage holographic photopolymers is illustrated in Scheme 1.

2.6. Fourier Transform Infrared Spectroscopy. FTIR was used to monitor the polymerization of the acrylate double bonds. A Thermo Scientific Nicolet 6700 FTIR spectrometer was electronically synchronized with a 405 nm light-emitting diode (LED) source (Thorlabs) using a myDAQ device (National Instruments), allowing for monitoring of the acrylate peak at 814 cm^{-1} with a timed and defined illumination at 16 mW/cm^2. Optically thin samples were prepared between two salt (NaCl) plates using 15 μm spacers. The stage 1 to stage 2 acrylate conversion ($C_{acrylate}$) was monitored using a series scan, integrating over the range 790−830 cm^{-1}, where $A_{initial}$ is the area of the unconsumed acrylate peak and A_{final} is the area under the acrylate peak after the stage 2 reaction.

$$C_{acrylate} = \left(1 - \frac{A_{final}}{A_{initial}}\right) \times 100\%$$

DOI: 10.1021/acsami.7b15063
ACS Appl. Mater. Interfaces 2018, 10, 1217−1224

2.7. Holographic Recording. A two-beam interference setup shown in Figure 1a was used to record volume transmission

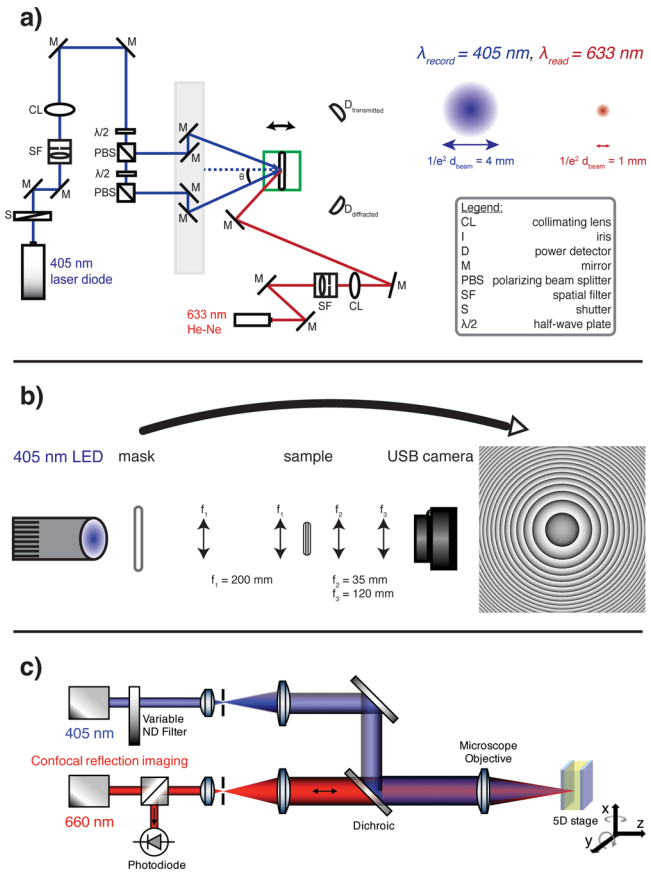

Figure 1. Optical recording schematics for systems used to record with 405 nm light: (a) volume transmission holograms recording sinusoidal diffraction gratings of 1 μm fringe spacing with a peak recording intensity of 16 mW/cm^2 of a Gaussian laser beam with a 1/e^2 diameter of 4.3 mm, (b) photomask lithography using a 1″ diameter Fresnel lens mask at an average recording intensity of 40 mW/cm^2, and (c) DLW of an image pattern with a peak recording intensity of ∼760 mW/cm^2 of a Gaussian beam with a 1/e^2 diameter of 10 μm.

holograms with a spatially filtered wavelength-stabilized 405 nm laser diode (Ondax, 40 mW). Both recording beams (1/e^2 intensity diameter of 4.3 mm) were power-matched to give a total recording intensity of ∼16 mW/cm^2. The beams were interfered at an external recording half-angle of 11.2° to produce a sinusoidal interference pattern with a fringe spacing of ∼1 μm. A 633 nm He−Ne laser (Thorlabs), aligned approximately at the Bragg reconstruction angle, was used as a read beam to nondestructively probe the hologram formation throughout the recording process. Each recording exposure is initially monitored for 300 s and then followed by a sample rotation from 15° to −15° at an angle increment of 0.05°. The optical power at both detectors was measured throughout the experiment. The diffraction efficiency of each recorded hologram was calculated by taking the quotient of the diffracted power (P_d) to the total power (transmitted + diffracted), DE = $I_d/(I_d + I_t)$. The diffraction efficiency versus angle profile was fitted to Kogelnik coupled wave theory[34] to obtain a peak-to-mean Δn and thickness (d).

2.8. Photolithography Mask Exposure. A projection lithography setup employing a 405 nm LED (Thorlabs—M405L3-C5) was used to expose a 1″ diameter Fresnel lens (1.5 diopter) pattern on a grayscale halftone chrome mask (Toppan Mask) as illustrated in Figure 1b.

2.9. Direct Laser Write. A 405 nm continuous wave laser with a focused spot (1/e^2 intensity diameter of 13 μm) is used to record isolated or continuous refractive index structures. The sample is mounted on a five-axis stage that controls both tip/tilt and xyz motion, whereas a coaligned confocal reflection microscope operating at 660 nm is used to align the sample as shown in Figure 1c.

3. RESULTS AND DISCUSSION

3.1. Monomer Structure and Synthesis. The goal of this work was to achieve a high Δn two-stage holographic material via an efficient writing monomer capable of a high refractive index after photopolymerization and significant loading into the matrix. The strategy to achieve this was through the design of a novel writing monomer capable of increased solubility in the urethane matrix without sacrificing the refractive index. A typical approach is to incorporate high refractive index groups via linker units to attach with the polymerizing functionality.[8] However, the linker units employed are usually alkyl chains, which reduce the overall refractive index of the monomer and polymer. To achieve this structure synthetically without the typical drawback in the refractive index, we employed a thiol−epoxy ring-opening reaction using a relatively high refractive index thiol, thiophenol (reported n_D = 1.588), and a substrate, epichlorohydrin, capable of further addition after the epoxide ring-opening reaction. With this in mind, the reaction was carried out with excess thiol under basic conditions so that after the initial ring-opening reaction of the epichlorohydrin, the chloro-substituted alcohol intermediate (1-chloro-3-(phenylthio)-2-propanol) that formed was able to further react with thiophenol to yield the desired symmetric diphenylthio-substituted secondary alcohol, BPTP, in a one-pot synthesis reaction. This molecular structure comprises advantageous characteristics for both refractive index and solubility. As outlined by the rearranged Lorentz−Lorenz equation[35]

$$n = \sqrt{\frac{1 + 2\left(\frac{[R]}{V}\right)}{1 - \left(\frac{[R]}{V}\right)}}$$

where n is the refractive index, $[R]$ is the molar refraction, and V is the molar volume. In BPTPA, the phenyl (N_A = 25.463), sulfur, and tertiary carbon moieties present are known high refractive index substituents with a high molar refraction relative to the molar volume.[36]

In terms of solubility, the flexible thioether linkages are known to freely form random molecular orientations and thus suppress packing between polymer chains. This linker unit is also especially beneficial for imparting a high refractive index in terms of sulfur content (21% for BPTPA) as well as for improving the solubility of the writing monomer/polymer within the polymer matrix. This behavior is evident by the measured refractive index of 1.62 (Abbe refractometer at 589.3 nm) for the colorless, low viscosity liquid BPTP precursor. Consistent properties are maintained even after the acylation reaction with acryloyl chloride which results in a colorless, low viscosity liquid with a refractive index of 1.6 (Abbe). The neat photopolymerized acrylate film using 1 mol % TPO registered a refractive index of 1.627 via prism coupler measurements at 633 nm.

To investigate further the viability and performance of BPTPA as a writing monomer, it was tested against a reference high refractive index writing monomer, TBPA. Given their

DOI: 10.1021/acsami.7b15063
ACS Appl. Mater. Interfaces 2018, 10, 1217−1224

comparable molecular weights, comparisons were done at equivalent weight percent compositions at 10 wt % increments. We encountered a solubility limitation at 50 wt % during formulation preparation whereby the monomer did not dissolve in the polyol to give a homogeneous and transparent resin. In contrast, BPTPA formulations containing up to 60 wt % writing monomer were successfully prepared.

3.2. Solubility of Writing Monomers in a Urethane Matrix. To assess the solubility capabilities of the writing monomer in a urethane matrix, we first determined the equilibrium mass uptake of the monomer in a nonsolvent (mineral oil) by the urethane matrix (Table 1) by measuring initial (W_i) and final weight (W_f). Approximately 50% more writing monomer (W_f/W_i) could be loaded into the matrix with BPTPA compared to TBPA. The quotient of the mass uptake of the writing monomer ($W_f - W_i$) with the final weight of the swollen matrix (W_f) was calculated to give a theoretical maximum loading of the writing monomer (in wt %).

Table 1. Swelling–Writing Monomer Mass Uptake by the Neat Polymeric Urethane Matrix

neat matrix	W_f/W_i[a]	$\Phi_{theoretical}$ (wt %)[b]
TBPA	1.94 ± 0.07	45 ± 2
BPTPA	2.94 ± 0.06	63 ± 1
control (no writing monomer)	1.03 ± 0.01	

[a]The ratio of the measured final weight (W_f) of the sample to its initial weight (W_i) was calculated. [b]Theoretical maximum loading (in wt %) was calculated by taking the ratio of the amount of mass uptake to its final weight, that is, $\Phi = (W_f - W_i)/W_f \times 100\%$.

3.3. Refractive Index of Two-Stage Formulations. To determine the expected refractive index increase per unit of the writing monomer present, the refractive indices of formulations containing varying amounts of the writing monomer were measured in their stage 1 and stage 2 (after UV flood exposure) state as shown in Figure 2. As is evident from the gradients of the linear fits for both stages 1 and 2, BPTPA demonstrates a higher Δn increase per unit of the writing monomer concentration (i.e., $\Delta n/[M]$). Using the gradient values for the linear fit equations, this $\Delta n/[M]$ increase is estimated to be approximately 20%. Therefore, assuming both monomers react similarly in rate and final conversion, a marginally higher Δn structure would be expected at equivalent monomer concentrations. More crucially, the ability to increase writing monomer loading extends the Δn ($n_{photopolymer} - n_{matrix}$) as shown by the dashed gray box inset of Figure 2.

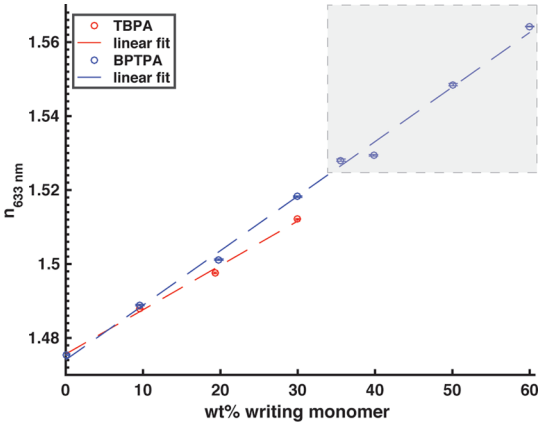

Figure 2. Final (stage 2) refractive indices of two-stage formulations for TBPA (red) and BPTPA (blue) as a function of the writing monomer content in weight percent. The gray dashed outline box in the upper right-hand corner specifies the accessible region for refractive index increase due to a higher solubility writing monomer.

3.4. Recording Kinetics. The photopolymerization reactivities of BPTPA and TBPA were assessed neat and as a stage 2 photopolymerization using 30 wt % writing monomer via real-time FTIR spectroscopy. Figure 3a shows that although TBPA has an almost instantaneous consumption of double bonds upon irradiation, it distinctly reaches a plateau of around 65% conversion due to vitrification. In the case of neat BPTPA, however, it has a slower initial rate but does in fact reach quantitative conversion within the exposure time of 20 s. This distinct polymerization kinetic profile is attributed to the lower viscosities throughout the polymerization of BPTPA. When these writing monomers are used in two-stage formulations, it is clear from Figure 3b that they both are indistinguishable in reactivity rates or final conversion (both quantitative). Therefore, the FTIR data suggest that BPTPA is at least comparable, if not preferable, to TBPA for its ability to go to full conversion at higher writing monomer loadings.

3.5. Holographic Recording (Transmission Gratings). Taking the solubility studies together with the refractive index measurements, we hypothesized a significant overall Δn recording improvement to be gained from enhancements in both $\Delta n/[M]$ and the amount of monomer that can be loaded. As a demonstration, high diffraction efficiency transmission volume holograms (fringe spacing $\Lambda \approx 1$ μm) were recorded from the TBPA and BPTPA samples at varying monomer loadings in thin films (<15 μm) to intentionally avoid overmodulation. Representative angular scans with good fits to Kogelnik coupled wave theory are shown in Figure 4a for samples containing 40, 50, and 60 wt % BPTPA with a peak-to-mean Δn of up to 0.029 demonstrated. Figure 4b shows the overall maximum achievable Δn for both writing monomers at increasing wt % loading. By increasing the writing monomer loading, we increase the observed Δn of a given material without a noticeable penalty in transparency or scatter. An additional advantage of the increased solubility of BPTPA is the boost in material sensitivity due to a concomitant increase in the polymerization rate that arises due to the higher monomer concentration.[37]

High sensitivity materials are especially critical for holography because of laser source limitations in power and overall setup stability time. This feature also extends to alternative photoinitiating systems which initiate at longer visible wavelengths but are less efficient.[9,10,31]

3.6. Bulk Δn versus Holographic Δn Analysis. Achievable holographic Δn in two-stage materials from a sinusoidal exposure is a fraction of the maximum achievable index response from a uniform flood cure. In fact, for a single holographic exposure (two-beam interference), it can be shown that the highest achievable Δn of the first harmonic is approximately 88% of a material's maximum refractive index response (see the Supporting Information). In Figure 5, the holographic Δn is plotted against the bulk Δn between stages 1 and 2 as measured using a prism coupler for both writing monomers. These results indicate that although BPTPA is able to achieve a higher holographic Δn through the increased

DOI: 10.1021/acsami.7b15063
ACS Appl. Mater. Interfaces 2018, 10, 1217–1224

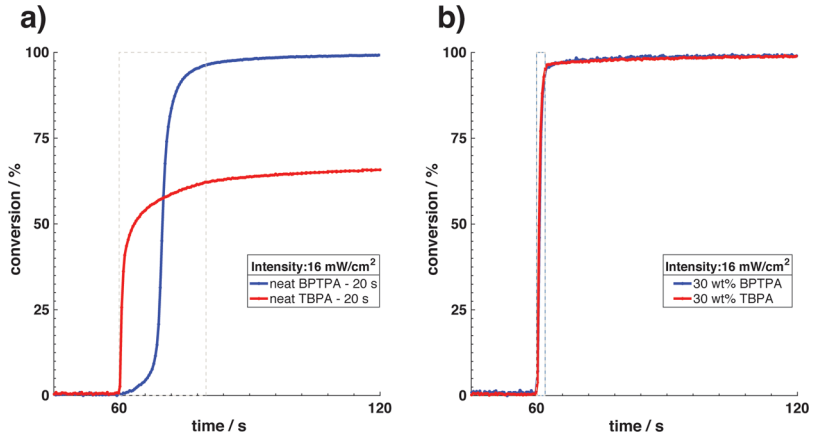

Figure 3. Real-time FTIR photopolymerization double bond conversion kinetics for the (a) neat acrylate (TBPA in red and BPTPA in blue) homopolymerization with 1 mol % TPO using triggered 405 nm LED irradiation (20 s at 16 mW/cm^2) at the 60 s mark and (b) acrylate homopolymerization of 30 wt % writing monomer (TBPA in red and BPTPA in blue) formulation with 10 mol % TPO using triggered 405 nm LED irradiation (2 s at 16 mW/cm^2) at the 60 s mark.

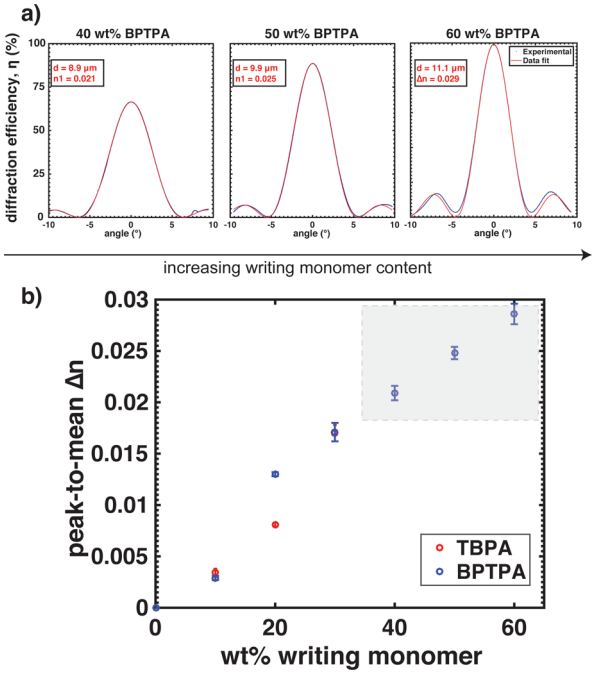

Figure 4. Transmission holography and Δn (peak-to-mean) values recorded with a pitch spacing of 1 μm at a recording intensity of 16 mW/cm^2 with exposure times of 1 s. (a) Representative diffraction efficiency vs reconstruction angle scans for 40, 50, and 60 wt % BPTPA formulations (data points in blue) with the corresponding fits (in red) to classical Kogelnik coupled wave theory. (b) Comparison of peak-to-mean Δn performance of TBPA against BPTPA as a function of the writing monomer content (TBPA in red; BPTPA in blue). The gray dashed outline box in the upper right-hand corner reveals the realized and achievable Δn increase from the higher solubility writing monomer BPTPA.

solubility, there is also a decrease in the "efficacy" of the increased index contrast at higher loadings.

3.7. Refractive Index Gradient Demonstrations.

Refractive index structures at low spatial frequencies are also demonstrated using the DLW of an arbitrary pattern and projection lithography using a Fresnel lens-etched chrome mask. The DLW example (Figure 6a) demonstrates distinct Δn between the photopolymer of BPTPA and the matrix while

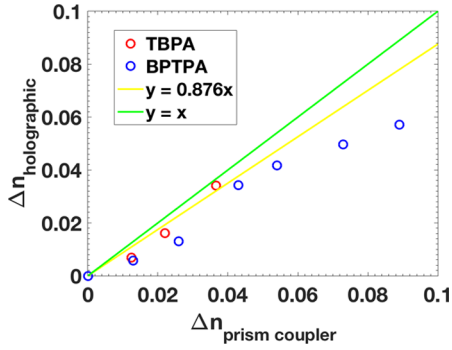

Figure 5. "Effective" Δn plot—achievable Δn with a sinusoidal intensity exposure measured via holography vs the achievable Δn in bulk measured via prism coupler for TBPA (in red) and BPTPA (in blue) at a varying writing monomer content. The green line specifies the ideal case for a perfect match between the Δn in bulk and holographic materials. The yellow line indicates the actual theoretical maximum Δn (88%) to be expected from the holographic Δn measured which only measures the first harmonic.

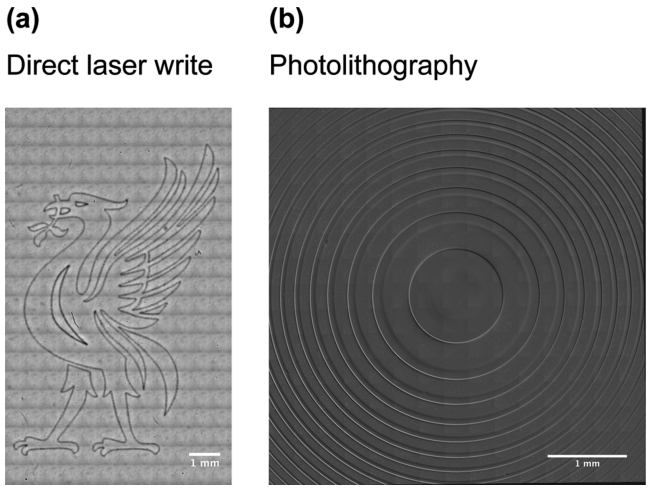

Figure 6. Demonstrative refractive index gradient examples. Stitched differential interference contrast (DIC) microscopy images of (a) DLW of a bird pattern and (b) projection mask lithography of a 1 in. diameter Fresnel lens.

DOI: 10.1021/acsami.7b15063
ACS Appl. Mater. Interfaces 2018, 10, 1217−1224

the Fresnel lens (Figure 6b) example validates the ability to record a structure with a fine gradient in refractive index. As evidenced by the stitched bright-field DIC microscopy (Nikon N-STORM) images in Figure 6, the material was able to record distinct submicron to tens of micron-sized features with excellent fidelity in both cases.

4. CONCLUSIONS

We report a novel acrylate monomer, BPTPA, that exhibits excellent properties. It is a highly reactive, colorless, liquid monomer with high refractive index that is readily synthesized from economical starting materials. This monomer was assessed for its solubility and refractive index change upon polymerization in a urethane matrix for use as a writing monomer in a two-stage formulation. BPTPA excelled over a reference, widely used high refractive index monomer, TBPA, on both measures allowing for formulations containing up to 60 wt % loading of BPTPA, which demonstrated a maximum $\Delta n \approx 0.029$ for volume transmission holograms. To the best of our knowledge, this value is the highest reported of any holographic photopolymer within the academic literature achieved with superior photosensitivity and simple synthetic preparation. This writing monomer and the synthetic protocol present promising avenues for the design of high refractive index writing monomers for high-performance holographic photopolymers.

■ ASSOCIATED CONTENT

Supporting Information

The Supporting Information is available free of charge on the ACS Publications website at DOI: 10.1021/acsami.7b15063.

NMR spectra of synthesized molecules, UV−vis spectra of two-stage formulations, and an explanation of maximum Δn from a single Bragg hologram exposure (PDF)

■ AUTHOR INFORMATION

Corresponding Authors

*E-mail: Robert.Mcleod@colorado.edu (R.R.M.).
*E-mail: Christopher.Bowman@colorado.edu (C.N.B.).

ORCID

Marvin D. Alim: 0000-0001-9983-3720
David J. Glugla: 0000-0002-6041-7751
Chen Wang: 0000-0003-0985-3221
Christopher N. Bowman: 0000-0001-8458-7723

Author Contributions

The manuscript was written through contributions of all authors. All authors have given approval to the final version of the manuscript. R.R.M. and C.N.B. share last authorship.

Funding

This material is based upon the work supported by Konica Minolta and the National Science Foundation under grant nos. ECCS 1307918 and DMR 1310528.

Notes

The authors declare no competing financial interest.

■ ACKNOWLEDGMENTS

The authors would like to thank Darren Forman, Jacob Friedlin, and Maciej Podgorski for their help and advice throughout the preparation of this manuscript. The imaging work was performed at the BioFrontiers Institute of Advanced Light Microscopy Core. Super resolution microscopy was performed on a Nikon N-STORM microscope supported by the Howard Hughes Medical Institute.

■ ABBREVIATIONS

HOE, holographic optical element; DLW, direct laser write; GRIN, gradient refractive index

■ REFERENCES

(1) Nair, D. P.; Cramer, N. B.; Gaipa, J. C.; McBride, M. K.; Matherly, E. M.; McLeod, R. R.; Shandas, R.; Bowman, C. N. Two-Stage Reactive Polymer Network Forming Systems. *Adv. Funct. Mater.* **2012**, *22*, 1502−1510.

(2) White, S. R.; Moore, J. S.; Sottos, N. R.; Krull, B. P.; Santa Cruz, W. A.; Gergely, R. C. R. Restoration of Large Damage Volumes in Polymers. *Science* **2014**, *344*, 620−623.

(3) Podgórski, M.; Nair, D. P.; Chatani, S.; Berg, G.; Bowman, C. N. Programmable Mechanically Assisted Geometric Deformations of Glassy Two-Stage Reactive Polymeric Materials. *ACS Appl. Mater. Interfaces* **2014**, *6*, 6111−6119.

(4) Toal, V. *Introduction to Holography*; CRC Press, 2012.

(5) Kowalski, B. A.; McLeod, R. R. Design Concepts for Diffusive Holographic Photopolymers. *J. Polym. Sci., Part B: Polym. Phys.* **2016**, *54*, 1021−1035.

(6) Dhar, L.; Hale, A.; Katz, H. E.; Schilling, M. L.; Schnoes, M. G.; Schilling, F. C. Recording Media That Exhibit High Dynamic Range for Digital Holographic Data Storage. *Opt. Lett.* **1999**, *24*, 487.

(7) Peng, H.; Nair, D. P.; Kowalski, B. A.; Xi, W.; Gong, T.; Wang, C.; Cole, M.; Cramer, N. B.; Xie, X.; McLeod, R. R.; Bowman, C. N. High Performance Graded Rainbow Holograms via Two-Stage Sequential Orthogonal Thiol−Click Chemistry. *Macromolecules* **2014**, *47*, 2306−2315.

(8) Peng, H.; Wang, C.; Xi, W.; Kowalski, B. A.; Gong, T.; Xie, X.; Wang, W.; Nair, D. P.; McLeod, R. R.; Bowman, C. N. Facile Image Patterning via Sequential Thiol−Michael/Thiol−Yne Click Reactions. *Chem. Mater.* **2014**, *26*, 6819−6826.

(9) Cody, D.; Gribbin, S.; Mihaylova, E.; Naydenova, I. Low-Toxicity Photopolymer for Reflection Holography. *ACS Appl. Mater. Interfaces* **2016**, *8*, 18481−18487.

(10) Ni, M.; Peng, H.; Liao, Y.; Yang, Z.; Xue, Z.; Xie, X. 3D Image Storage in Photopolymer/ZnS Nanocomposites Tailored by "Photo-initibitor.". *Macromolecules* **2015**, *48*, 2958−2966.

(11) Tomita, Y.; Urano, H.; Fukamizu, T.-a.; Kametani, Y.; Nishimura, N.; Odoi, K. Nanoparticle-Polymer Composite Volume Holographic Gratings Dispersed with Ultrahigh-Refractive-Index Hyperbranched Polymer as Organic Nanoparticles. *Opt. Lett.* **2016**, *41*, 1281−1284.

(12) Peng, H.; Bi, S.; Ni, M.; Xie, X.; Liao, Y.; Zhou, X.; Xue, Z.; Zhu, J.; Wei, Y.; Bowman, C. N.; Mai, Y.-W. Monochromatic Visible Light "Photoinitibitor": Janus-Faced Initiation and Inhibition for Storage of Colored 3D Images. *J. Am. Chem. Soc.* **2014**, *136*, 8855−8858.

(13) Choi, K.; Chon, J. W. M.; Gu, M.; Malic, N.; Evans, R. A. Low-Distortion Holographic Data Storage Media Using Free-Radical Ring-Opening Polymerization. *Adv. Funct. Mater.* **2009**, *19*, 3560−3566.

(14) Urness, A. C.; Anderson, K.; Ye, C.; Wilson, W. L.; McLeod, R. R. Arbitrary GRIN Component Fabrication in Optically Driven Diffusive Photopolymers. *Opt. Express* **2015**, *23*, 264−273.

(15) Sullivan, A. C.; Grabowski, M. W.; McLeod, R. R. Three-Dimensional Direct-Write Lithography into Photopolymer. *Appl. Opt.* **2007**, *46*, 295.

(16) Yee, D. W.; Schulz, M. D.; Grubbs, R. H.; Greer, J. R. Functionalized 3D Architected Materials via Thiol-Michael Addition and Two-Photon Lithography. *Adv. Mater.* **2017**, *29*, 1605293.

(17) Kress, B. C. *Restocking the Optical Designers' Toolbox for Next-Generation Wearable Displays (Presentation Recording)*; Gregory, G. G., Davis, A. J., Hahlweg, C. F., Eds.; International Society for Optics and Photonics, 2015; p 957903.

DOI: 10.1021/acsami.7b15063
ACS Appl. Mater. Interfaces 2018, 10, 1217−1224

(18) Bruder, F.-K.; Hagen, R.; Rölle, T.; Weiser, M.-S.; Fäcke, T. From the Surface to Volume: Concepts for the Next Generation of Optical-Holographic Data-Storage Materials. *Angew. Chem., Int. Ed.* **2011**, *50*, 4552−4573.
(19) Kowalski, B. A.; Urness, A. C.; Baylor, M.-E.; Cole, M. C.; Wilson, W. L.; McLeod, R. R. Quantitative Modeling of the Reaction/diffusion Kinetics of Two-Chemistry Diffusive Photopolymers. *Opt. Mater. Express* **2014**, *4*, 1668.
(20) Higashihara, T.; Ueda, M. Recent Progress in High Refractive Index Polymers. *Macromolecules* **2015**, *48*, 1915−1929.
(21) Liu, J.-g.; Ueda, M. High Refractive Index Polymers: Fundamental Research and Practical Applications. *J. Mater. Chem.* **2009**, *19*, 8907−8919.
(22) Macdonald, E. K.; Shaver, M. P. Intrinsic High Refractive Index Polymers. *Polym. Int.* **2015**, *64*, 6−14.
(23) Gharagheizi, F.; Ilani-Kashkouli, P.; Kamari, A.; Mohammadi, A. H.; Ramjugernath, D. Group Contribution Model for the Prediction of Refractive Indices of Organic Compounds. *J. Chem. Eng. Data* **2014**, *59*, 1930−1943.
(24) Meka, C.; Jallapuram, R.; Naydenova, I.; Martin, S.; Toal, V. Development of a Panchromatic Acrylamide-Based Photopolymer for Multicolor Reflection Holography. *Appl. Opt.* **2010**, *49*, 1400−1405.
(25) Liu, S.; Gleeson, M. R.; Guo, J.; Sheridan, J. T. High Intensity Response of Photopolymer Materials for Holographic Grating Formation. *Macromolecules* **2010**, *43*, 9462−9472.
(26) Bunning, T. J.; Natarajan, L. V.; Tondiglia, V. P.; Sutherland, R. L. Holographic Polymer-Dispersed Liquid Crystals (H-PDLCs). *Annu. Rev. Mater. Sci.* **2000**, *30*, 83−115.
(27) Bunning, T. The Morphology and Performance of Holographic Transmission Gratings Recorded in Polymer Dispersed Liquid Crystals. *Polymer* **1995**, *36*, 2699−2708.
(28) White, T. J.; Natarajan, L. V.; Tondiglia, V. P.; Lloyd, P. F.; Bunning, T. J.; Guymon, C. A. Monomer Functionality Effects in the Formation of Thiol−Ene Holographic Polymer Dispersed Liquid Crystals. *Macromolecules* **2007**, *40*, 1121−1127.
(29) Natarajan, L. V.; Shepherd, C. K.; Brandelik, D. M.; Sutherland, R. L.; Chandra, S.; Tondiglia, V. P.; Tomlin, D.; Bunning, T. J. Switchable Holographic Polymer-Dispersed Liquid Crystal Reflection Gratings Based on Thiol−Ene Photopolymerization. *Chem. Mater.* **2003**, *15*, 2477−2484.
(30) Sutherland, R. L.; Tondiglia, V. P.; Natarajan, L. V.; Bunning, T. J. Evolution of Anisotropic Reflection Gratings Formed in Holographic Polymer-Dispersed Liquid Crystals. *Appl. Phys. Lett.* **2001**, *79*, 1420.
(31) Chen, G.; Ni, M.; Peng, H.; Huang, F.; Liao, Y.; Wang, M.; Zhu, J.; Roy, V. A. L.; Xie, X. Photoinitiation and Inhibition under Monochromatic Green Light for Storage of Colored 3D Images in Holographic Polymer-Dispersed Liquid Crystals. *ACS Appl. Mater. Interfaces* **2017**, *9*, 1810−1819.
(32) Bruder, F.-K.; Fäcke, T.; Rölle, T. The Chemistry and Physics of Bayfol HX Film Holographic Photopolymer. *Polymers* **2017**, *9*, 472.
(33) Ayres, M. R.; Anderson, K.; Askham, F.; Sissom, B.; Urness, A. C. *Holographic Data Storage at 2+ Tbit/in* $_2$; Bjelkhagen, H. I., Bove, V. M., Eds.; International Society for Optics and Photonics, 2015; Vol. *9386*, p 93860G.
(34) Kogelnik, H. Coupled Wave Theory for Thick Hologram Gratings. *Bell Syst. Tech. J.* **1969**, *48*, 2909−2947.
(35) Heller, W. Remarks on Refractive Index Mixture Rules. *J. Phys. Chem.* **1965**, *69*, 1123−1129.
(36) Groh, W.; Zimmermann, A. What is the Lowest Refractive Index of an Organic Polymer? *Macromolecules* **1991**, *24*, 6660−6663.
(37) Odian, G. *Principles of Polymerization*; Wiley-Interscience: New York, 1991.

DOI: 10.1021/acsami.7b15063
ACS Appl. Mater. Interfaces 2018, 10, 1217−1224